Letter

Non-Hermitian skin effects on thermal and many-body localized phases

Yi-Cheng Wang,[1,2,*] Kuldeep Suthar,[1,3,*] H. H. Jen,[1,4] Yi-Ting Hsu,[5,†] and Jhih-Shih You[6,‡]

[1]*Institute of Atomic and Molecular Sciences, Academia Sinica, Taipei 10617, Taiwan*
[2]*Department of Physics, National Taiwan University, Taipei 10617, Taiwan*
[3]*Department of Physics, Central University of Rajasthan, Ajmer 305817, Rajasthan, India*
[4]*Physics Division, National Center for Theoretical Sciences, Taipei 10617, Taiwan*
[5]*Department of Physics, University of Notre Dame, Notre Dame, Indiana 46556, USA*
[6]*Department of Physics, National Taiwan Normal University, Taipei 11677, Taiwan*

(Received 31 January 2023; revised 13 June 2023; accepted 13 June 2023; published 26 June 2023)

Localization in one-dimensional interacting systems can be caused by disorder potentials or non-Hermiticity. The former phenomenon is the many-body localization (MBL), and the latter is the many-body non-Hermitian skin effect (NHSE). In this work, we numerically investigate the interplay between these two kinds of localization, where the energy-resolved MBL arises from a deterministic quasiperiodic potential in a fermionic chain. We propose a set of eigenstate properties and long-time dynamics that collectively distinguish the two localization mechanisms in the presence of non-Hermiticity. By computing the proposed diagnostics, we show that the thermal states are vulnerable to the many-body NHSE while the MBL states remain resilient up to a strong non-Hermiticity. Finally, we discuss experimental observables that probe the difference between the two localizations in a non-Hermitian quasiperiodic fermionic chain. Our results pave the way toward experimental observations on the interplay of interaction, quasiperiodic potential, and non-Hermiticity.

DOI: 10.1103/PhysRevB.107.L220205

I. INTRODUCTION

Many-body localization (MBL) [1–3] can exist in one-dimensional (1D) isolated quantum systems in the presence of interaction and disorders, where thermalization fails to take place [4–7] and the information encoded in the initial state is preserved [8–10]. Besides the well-known cases with random disorders [5,6,11–15], where the thermal-to-MBL transition occurs as the disorder strength increases, numerical [16–27] and experimental [8,28,29] evidences have suggested that MBL can also occur in the presence of deterministic but quasiperiodic potentials. In particular, in quasiperiodic systems with a single-particle mobility edge, MBL and thermal phases coexist at a given intermediate potential strength in low- and midspectrum regimes, respectively [17–20]. Such an energy-resolved localization-delocalization transition originates from the nontrivial interplay between the interaction and quasiperiodic potential, where the latter provides a localization mechanism in many-body Hermitian systems.

In non-Hermitian systems, a distinct localization mechanism dubbed the non-Hermitian skin effect (NHSE) has recently attracted rapidly growing theoretical [30–44] and experimental [45–54] attention, where an extensive number of eigenstates are localized at open boundaries. In the noninteracting limit, single-particle NHSE occurs under open-boundary conditions when the eigenspectrum under periodic boundary condition exhibits nontrivial winding [37,38]. In specific models, such winding and localization can occur when non-Hermiticity is introduced by nonreciprocal hoppings [55]. In the presence of interactions, although the relation between the winding in the eigenspectrum and many-body NHSE remains an interesting but elusive topic, recent theoretical works have investigated the existence [56,57] and entanglement dynamics [58] of many-body NHSE in fermionic systems, how MBL is affected by non-Hermiticity [59,60], as well as NHSE in random disordered systems [61]. Although the many-body NHSE does not exhibit strictly exponential localization in real space as the single-particle NHSE does due to the Pauli exclusion principle [57], particles in all the many-body eigenstates are still expected to accumulate on one end of open boundaries in the strong non-Hermiticity limit. Therefore, in stark contrast to MBL, where particles in a given initial state stay localized at their initial positions, many-body NHSE tends to push all particles towards one of the open boundaries such that the initial information is lost. Yet, the competition between these two localizations in interacting 1D systems with both non-Hermiticity and quasiperiodic potentials remains elusive.

In this Letter, we investigate how many-body NHSE affects the MBL and thermal phases in 1D quasiperiodic systems, focusing on a case study of the generalized Aubry-André (GAA) model [17,18,62,63] in the presence of nonreciprocal hopping. To distinguish the two localization mechanisms, we propose a set of eigenstate properties and dynamical responses that can collectively diagnose the many-body NHSE and the non-Hermitian localized phase connected to the Hermitian MBL, dubbed non-Hermitian MBL. Our key finding

*These authors contributed equally to this work.
†Corresponding author: yhsu2@nd.edu
‡Corresponding author: jhihshihyou@ntnu.edu.tw

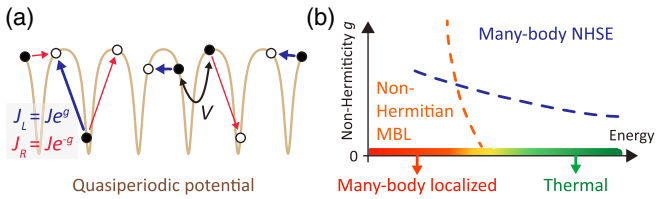

FIG. 1. (a) Schematic of an open fermionic chain subject to a generalized Aubry-André potential (brown, $\phi = 0$). The nonreciprocal hopping $J_{L(R)} = Je^{\pm g}$ (blue and red) and nearest-neighbor interaction V (black) are shown according to the configuration of occupied (•) and unoccupied (○) sites. (b) The phase diagram as a function of energy and the non-Hermiticity parameter g explored in this Letter. The red and blue dashed lines roughly separate the parameter regimes for initial state memory and localization of particles at the open boundary, respectively.

is that the thermal phase is vulnerable to non-Hermiticity such that the volume-law entanglement entropy vanishes and the many-body NHSE appears already at a small asymmetry between the left and right hopping. In contrast to the thermal phase, MBL dominates over the many-body NHSE up to an extremely large hopping asymmetry, where the many-body eigenstates across the full spectrum exhibit strong NHSE. Importantly, we emphasize that although both quasiperiodic potentials and non-Hermiticity can drive localization, the many-body NHSE does *not* preserve the information of the initial state as does the MBL phase. Finally, we discuss a possible experimental detection scheme that distinguishes non-Hermitian MBL and many-body NHSE by using the long-time behaviors of generalized imbalance [64–66] and local particle numbers, respectively. We expect that our observation of how the many-body NHSE affects the thermal and MBL phases is generic for other non-Hermitian systems with many-body NHSE in the presence of quasiperiodic as well as random disorder potentials.

II. MODEL

In the absence of interactions, models with nonreciprocal hoppings are well known to exhibit winding in the eigenspectrum and thus single-particle NHSE, and could be realized experimentally in various systems [67–69]. Now in the presence of interactions, we therefore investigate many-body NHSE by introducing non-Hermiticity with nonreciprocal hoppings. Specifically, we consider a non-Hermitian interacting GAA model that has a nonreciprocal factor $e^{\pm g}$ in the nearest-neighbor hopping terms [Fig. 1(a)]

$$H = \sum_{j=1}^{L-1}[-J(e^{g}c_j^\dagger c_{j+1} + e^{-g}c_{j+1}^\dagger c_j) + Vn_jn_{j+1}] + \sum_{j=1}^{L} 2\lambda \frac{\cos(2\pi qj+\phi)}{1-\alpha\cos(2\pi qj+\phi)} n_j, \quad (1)$$

where $c_j^\dagger$ creates a fermion on site j in an open chain with L sites, $n_j = c_j^\dagger c_j$ is the density operator, V is the nearest-neighbor density-density interaction, and $g \neq 0$ controls the strength of non-Hermiticity. The model has a quasiperiodic potential with strength 2λ, an irrational wave number $q = (\sqrt{5}-1)/2$, a randomly chosen global phase ϕ, and a dimensionless parameter $\alpha = -0.8$ that controls the potential shape. In the noninteracting limit, this model exhibits an exact single-particle mobility edge at energy $E = 2\mathrm{sgn}(\lambda)(|J| - |\lambda|)/\alpha$ [62]. At nonzero interaction, previous numerical studies [17,20] on a Hermitian GAA model ($g = 0$) with a moderate potential strength found MBL and thermal states in the low- and midspectrum regimes, respectively, along with an intermediate phase between them [Fig. 1(b)]. In the following, we choose $V/J = 1$ and $\lambda/J = 0.45$ such that both MBL and thermal states exist at the low- and midspectrum regimes in the Hermitian limit $g = 0$, respectively.

III. NON-HERMITICITY INDUCED LOCALIZATION: NHSE

To investigate the role of non-Hermiticity in an interacting quasiperiodic system, we first note that the eigenspectrum of Eq. (1) is independent of g regardless of total particle number. This is because it can be mapped from a Hermitian GAA model by the imaginary gauge transformation [55]. We note that adding an imaginary gauge in the momentum-space Hamiltonian, $H = \sum_k H_k c_k^\dagger c_k \to \sum_k H_{k-ig} c_k^\dagger c_k$, is equivalent to the transformation on the annihilation and creation operators, $c_k \to c_{k+ig}$ and $c_k^\dagger \to c_{k+ig}^\dagger$. The corresponding real-space representations are $c_j \to e^{gj}c_j$ and $c_j^\dagger \to e^{-gj}c_j^\dagger$. As a result, the level spacing statistics, a commonly used diagnostic that indicates the MBL and thermal phases in the Hermitian system [5,16], cannot reflect the occurrence of NHSE or the fate of MBL and thermal states at $g \neq 0$ [70]. Nevertheless, we expect that the influence of NHSE can be identified from eigenstate-related quantities since the probability of many-body product states $|n\rangle$ with particles accumulated near one of the open ends is enhanced as $|n\rangle \to e^{-g\sum_{j=1}^{L} jn_j}|n\rangle$, followed by normalization. We therefore investigate two eigenstate properties in the following to capture the impact of NHSE.

The two eigenstate-based quantities we study are the energy-resolved real-space local density $\langle n_j\rangle$ and Rényi entropy $S_2(l,L) = -\log[\mathrm{Tr}\rho_A^2]$, where $\rho_A = \mathrm{Tr}_B[|\psi\rangle\langle\psi|]$ is the reduced density matrix of eigenstate $|\psi\rangle$ for the left subsystem A that consists of sites $i = 1, 2, \ldots, l \leqslant L$ in an L-site open chain, obtained by tracing out the right subsystem B. Both energy-resolved quantities are computed by eigenstates uniformly sampled throughout the spectrum using exact diagonalization (ED) for an $L = 30$ chain with $N = 5$ particles. Since the eigenenergies remain unchanged under the non-Hermiticity magnitude g, we can study how $\langle n_j\rangle$ and $S_2(l,L)$ at different energies change from the Hermitian $g = 0$ to the non-Hermitian $g > 0$ cases.

We first show the drastic energy dependence in how the real-space local density $\langle n_j\rangle$ evolves with the non-Hermiticity g [see Fig. 2(a)]. At $g = 0$ in the left panel, the low- and midspectrum eigenstates show symmetric $\langle n_j\rangle$ with respect to the center of the 1D chain, such that any asymmetric local density at nonzero g reflects the influence of NHSE. As we turn on the non-Hermiticity at $g = 0.5$ in the right panel, the midspectrum eigenstates become localized on the left end

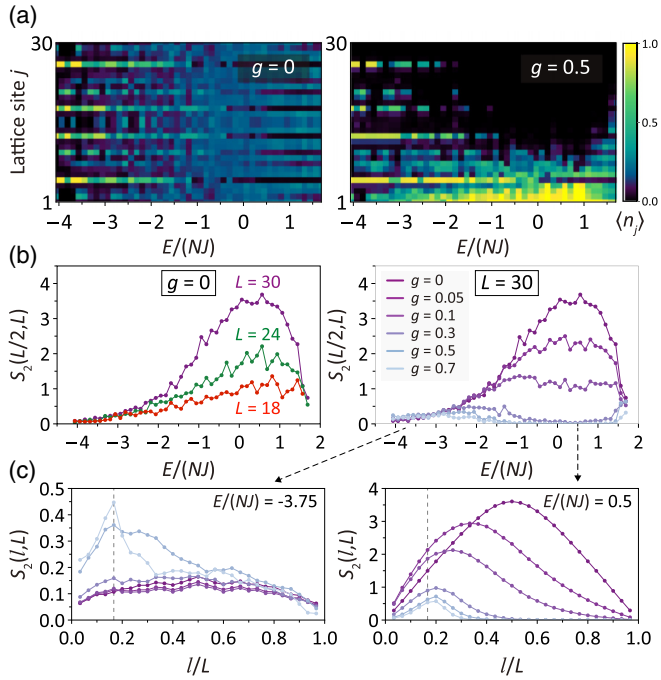

FIG. 2. (a) Energy-resolved local particle numbers in real space for Hermitian (left, $g = 0$) and non-Hermitian (right, $g = 0.5$) cases. (b) In the Hermitian case (left), eigenstates exhibit area-law and volume-law entanglement scalings in the low- and midspectrum regimes, respectively. The nonreciprocal hoppings (right) result in entanglement reduction in the midspectrum regime. (c) Rényi entropy as a function of subsystem size l at low- (left, MBL at $g = 0$) and midspectrum (right, thermal at $g = 0$) regimes. The color gradient follows that in the right panel of (b), and the dashed vertical line indicates $l/L = N/L$. The plots are obtained by averaging over ϕ [70], and filling $N/L = 1/6$ is considered throughout this work.

while the low-spectrum eigenstates are only slightly affected. This non-Hermiticity induced localization on the left end in the midspectrum eigenstates suggests many-body NHSE, and the sharp contrast between the low- and midspectrum regimes suggests that the thermal eigenstates (midspectrum) are much more vulnerable to the many-body NHSE than the MBL eigenstates (low spectrum).

The same behavior is observed in the g dependence in the energy resolved half-chain Rényi entropies $S_2(L/2, L)$ [see Fig. 2(b)]. At $g = 0$ in the left panel, the low- and midspectrum eigenstates exhibit area-law and volume-law [71] entanglement scalings, respectively, as expected from the MBL and thermal phases. In the presence of non-Hermiticity $g > 0$ at different degrees (see the right panel), the half-chain entanglement of midspectrum eigenstates decreases drastically with g, showing that many-body eigenstates become localized due to many-body NHSE. In contrast, the low-energy half-chain entanglement entropies remain resilient within the range shown here, and will not be significantly affected by NHSE until an extremely large g is reached [70].

Finally, we show that the subsystem-size l dependence of $S_2(l, L)$ is in fact a more sensitive diagnostic for the influence of many-body NHSE in the thermal and MBL energy regimes [see Fig. 2(c)]. At $g = 0$, the representative MBL and thermal states in the left and right panels, respectively, show area-law scaling and universal volume-law behavior [72]. At small $g > 0$, it is evident that the thermal state already exhibits a significant change in $S_2(l, L)$ at a small g, while the $S_2(l, L)$ of the MBL state remain unchanged. Nonetheless, both thermal and MBL states manifest NHSE at a strong non-Hermiticity $g = 0.7$, where $S_2(l, L)$ are asymmetric and peak at $l/L = N/L = 1/6$. This is expected for NHSE because all particles are accumulated on the left end at large enough g regardless of the energy regime, where the nonzero entanglement can only build up for subsystem size l/L in the vicinity of N/L [70]. The filling N/L-controlled asymmetric behavior in the subsystem-size l dependence of Rényi entropy $S_2(l, L)$ therefore serves as a sensitive diagnostic for many-body NHSE.

IV. DYNAMICAL PROPERTIES AND EXPERIMENTAL OBSERVABLES

The fate of MBL in the non-Hermitian GAA model can be revealed from the hallmark of MBL: initial state memory retention. To describe the non-Hermitian dynamics, we compute the time evolution by the quantum trajectory formalism under no-jump condition [73], which corresponds to continuously measured systems or postselection. We take product states in an $L = 18$ open chain with $N = 3$ particles as the initial states $|\psi_0\rangle$. At time t, the state is given by $|\psi_t\rangle = e^{-iHt}|\psi_0\rangle/\sqrt{\langle\psi_0|e^{iH^\dagger t}e^{-iHt}|\psi_0\rangle}$. Note that the non-Hermiticity results in an energy nonconservation process. Nonetheless, we can characterize different initial states by their steady-state energies at long times [70].

We start by choosing the initial product states whose real parts of long-time energies are in the low- and midspectrum regimes, where the former and latter are considered to be in the MBL and thermal phases at $g = 0$. Figure 3(a) shows the time evolution of local density. In the low-spectrum regime (left), the persisting memory of the initial state at $g = 0$ (top) and $g = 0.15$ (bottom) breaks ergodicity and is consistent with the features of MBL. Here we consider different ϕ and different initial states such that the top and bottom plots possess the same long-time energy. In the midspectrum regime (right), on the contrary, the initial product state rapidly spreads over the whole lattice at $g = 0$ (top), reflecting the absence of initial-state memory. At $g = 0.15$ (bottom), although the initial information is lost within a short time frame, the long-time dynamics of the system still exhibits a non-Hermiticity induced localization at the left end.

The preservation of initial information can be better expressed as the generalized imbalance [64–66]

$$\hat{\mathcal{I}}_{\text{gen}} = \sum_{j=1}^{L} \beta_j n_j, \tag{2}$$

where $\beta_j = N^{-1}$ and $-(L-N)^{-1}$ for initially occupied and unoccupied sites, respectively, when $N < L/2$. This ensures that all initial product states $|\psi_0\rangle$ have unity generalized imbalance, i.e., $\langle\psi_0|\hat{\mathcal{I}}_{\text{gen}}|\psi_0\rangle = 1$. For a delocalized phase where a particle occupies any site with equal probability, $\langle\psi_t|\hat{\mathcal{I}}_{\text{gen}}|\psi_t\rangle$ would relax to zero at long times, while for the perfect preservation $\langle\psi_t|\hat{\mathcal{I}}_{\text{gen}}|\psi_t\rangle \to 1$. Here we choose the value of $\mathcal{I}_{\text{gen}} = (N/2)N^{-1} - (N/2)(L-N)^{-1}$, which roughly

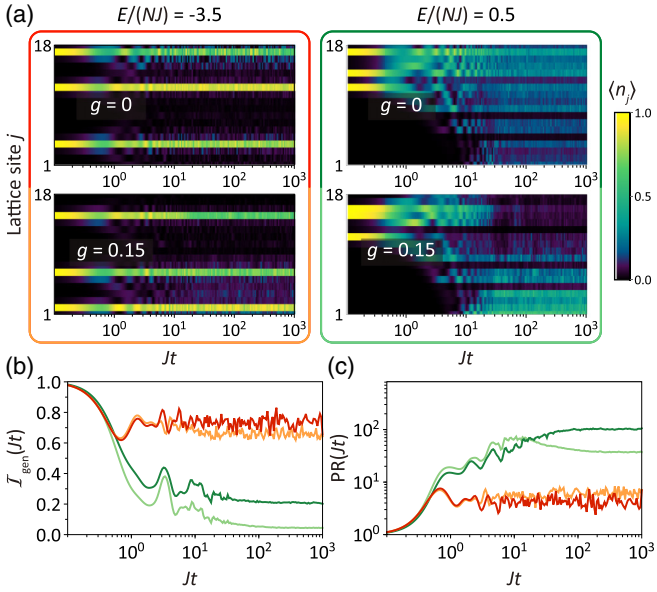

FIG. 3. (a) Site-resolved dynamics of initial product states with low (left) and high (right) real parts of energies at long times. The global phases $\phi + \pi q(L+1)$, which are defined modulo 2π, are chosen as left: 1.9π (top) and 0.4π (bottom) and right: 0.7π (top) and 0.7π (bottom). (b and c) Dynamics of (b) generalized imbalance $\mathcal{I}_{\text{gen}}$ and (c) participation ratio PR at low- (orange) and midspectrum (green) regimes in the Hermitian (dark) and non-Hermitian (light). The parameters used in each curve follow the corresponding color of the boundary line in (a).

separates the MBL phase from other phases, under the assumption that a particle has equal probability to populate the initially occupied and unoccupied sites. In our case, the $N/L = 1/6$ filling corresponds to $\mathcal{I}_{\text{gen}} = 0.4$. Figure 3(b) shows that the generalized imbalance at long times exhibits the initial-state memory retention in the low-spectrum regime, which indicates MBL.

To visualize the localization in the Fock space from the dynamics, we consider the participation ratio $\text{PR}(Jt) = [\sum_{n=1}^{\mathcal{D}_{N,L}} |\langle n|\psi_t\rangle|^4]^{-1}$, where $|n\rangle$ is a product state and $\mathcal{D}_{N,L} = L!/[(L-N)!N!]$ is the dimension of Hilbert space in the N particle sector. In a uniformly distributed state, PR corresponds to upper bound $\mathcal{D}_{N,L}$, while a localized state has a relatively small PR. In Fig. 3(c), we find that in the midspectrum regime the nonreciprocal hopping ($g = 0.15$) can suppress PR at long-time. Therefore, in this regime non-Hermiticity can prevent a state from traversing the whole Hilbert space but cannot preserve initial information.

V. THE PHASE DIAGRAMS OF MBL AND MANY-BODY NHSE

We can establish the phase diagrams of MBL and many-body NHSE by a set of experimentally feasible quantities. The left panel in Fig. 4(a) presents the generalized imbalance at $Jt = 1000$ as a function of the real part of energy. The MBL phase is characterized by the parameter region with $\mathcal{I}_{\text{gen}} > 0.4$, which is shown in red with a dashed blue line as a guide to the eye. These results suggest that the

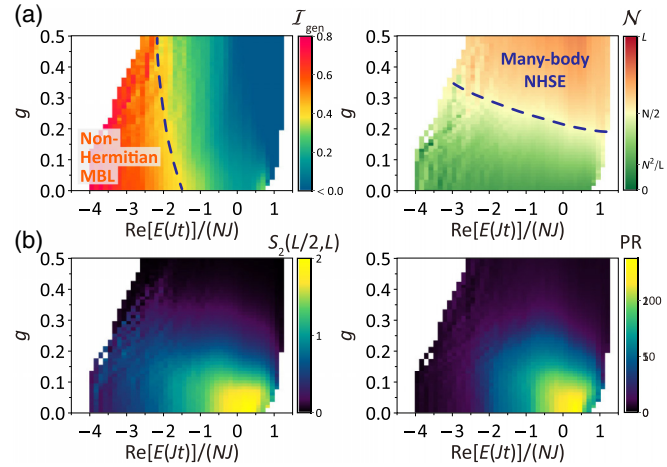

FIG. 4. Snapshots of (a) generalized imbalance $\mathcal{I}_{\text{gen}}$ (left) and number of particles at the first N sites $\mathcal{N}$ (right) and (b) half-chain Rényi entropy $S_2(L/2, L)$ (left) and participation ratio PR (right) at $Jt = 1000$. $L = 18$ is considered in these plots.

parameter region of MBL would be slightly affected by the non-Hermiticity g, which cannot be revealed by the level statistics.

To characterize the many-body NHSE, we calculate the total particle numbers at the first N sites $\mathcal{N}(Jt) = \langle\psi_t|\sum_{j=1}^{N} n_j|\psi_t\rangle$ at a long time. In the absence of NHSE, $\mathcal{N}$ is expected to be N^2/L, shown at $g = 0$ in the right panel of Fig. 4(a). In the strong g limit, $\mathcal{N}$ would approach N, such that $\mathcal{N} = N/2$ (indicated by a dashed blue line) is a good reference value to characterize the many-body NHSE. It is evident that states with higher $\text{Re}[E(Jt)]/(NJ)$ are more vulnerable to NHSE, which is consistent with Fig. 2(b). At large g, both extended and localized phases are dominated by the many-body NHSE. In Fig. 4(b), we show that the long-time half-chain Rényi entropy and participation ratio have a similar pattern. Thus, non-Hermitian MBL and many-body NHSE can be well defined by the large long-time generalized imbalance and by the accumulation of particles at the open boundary, respectively, from which the phase diagram in Fig. 1(b) is established.

VI. CONCLUSION

We have shown that NHSE has a significant impact on thermal states, while MBL states require strong non-Hermiticity to be altered. These features are manifested in both many-body eigenstates and quench dynamics of product states. Here we focus on the distinct behaviors of individual phases, while their separations and intermediate stages require further studies. Based on the experimentally feasible quantities we provided, we expect our analysis can be applied to generic interacting non-Hermitian systems with random disorder or quasiperiodic potential.

ACKNOWLEDGMENTS

We thank Qian-Rui Huang and Po-Jen Hsu for technical support. We also thank Sankar Das Sarma for comments

on the manuscript. Y.-C.W., K.S., and H.H.J. acknowledge support from the Ministry of Science and Technology (MOST), Taiwan, under Grant No. MOST-109-2112-M-001-035-MY3. Y.-C.W. and J.-S.Y. are supported by the Ministry of Science and Technology, Taiwan (Grant No. MOST-110-2112-M-003-008-MY3). H.H.J. and J.-S.Y. are also grateful for support from the National Center for Theoretical Sciences in Taiwan.

[1] R. Nandkishore and D. A. Huse, Many-body localization and thermalization in quantum statistical mechanics, Annu. Rev. Condens. Matter Phys. **6**, 15 (2015).

[2] F. Alet and N. Laflorencie, Many-body localization: An introduction and selected topics, C. R. Phys. **19**, 498 (2018).

[3] D. A. Abanin, E. Altman, I. Bloch, and M. Serbyn, Colloquium: Many-body localization, thermalization, and entanglement, Rev. Mod. Phys. **91**, 021001 (2019).

[4] D. M. Basko, I. L. Aleiner, and B. L. Altshuler, Possible experimental manifestations of the many-body localization, Phys. Rev. B **76**, 052203 (2007).

[5] V. Oganesyan and D. A. Huse, Localization of interacting fermions at high temperature, Phys. Rev. B **75**, 155111 (2007).

[6] A. Pal and D. A. Huse, Many-body localization phase transition, Phys. Rev. B **82**, 174411 (2010).

[7] M. Serbyn, Z. Papić, and D. A. Abanin, Local Conservation Laws and the Structure of the Many-Body Localized States, Phys. Rev. Lett. **111**, 127201 (2013).

[8] M. Schreiber, S. S. Hodgman, P. Bordia, H. P. Lüschen, M. H. Fischer, R. Vosk, E. Altman, U. Schneider, and I. Bloch, Observation of many-body localization of interacting fermions in a quasirandom optical lattice, Science **349**, 842 (2015).

[9] Jae-yoon Choi, S. Hild, J. Zeiher, P. Schauß, A. Rubio-Abadal, T. Yefsah, V. Khemani, D. A. Huse, I. Bloch, and C. Gross, Exploring the many-body localization transition in two dimensions, Science **352**, 1547 (2016).

[10] J. Smith, A. Lee, P. Richerme, B. Neyenhuis, P. W. Hess, P. Hauke, M. Heyl, D. A. Huse, and C. Monroe, Many-body localization in a quantum simulator with programmable random disorder, Nat. Phys. **12**, 907 (2016).

[11] I. V. Gornyi, A. D. Mirlin, and D. G. Polyakov, Interacting Electrons in Disordered Wires: Anderson Localization and Low-t Transport, Phys. Rev. Lett. **95**, 206603 (2005).

[12] D. M. Basko, I. L. Aleiner, and B. L. Altshuler, Metal-insulator transition in a weakly interacting many-electron system with localized single-particle states, Ann. Phys. **321**, 1126 (2006).

[13] M. Žnidarič, T. Prosen, and P. Prelovšek, Many-body localization in the Heisenberg *XXZ* magnet in a random field, Phys. Rev. B **77**, 064426 (2008).

[14] J. A. Kjäll, J. H. Bardarson, and F. Pollmann, Many-Body Localization in a Disordered Quantum Ising Chain, Phys. Rev. Lett. **113**, 107204 (2014).

[15] D. J. Luitz, N. Laflorencie, and F. Alet, Many-body localization edge in the random-field Heisenberg chain, Phys. Rev. B **91**, 081103(R) (2015).

[16] S. Iyer, V. Oganesyan, G. Refael, and D. A. Huse, Many-body localization in a quasiperiodic system, Phys. Rev. B **87**, 134202 (2013).

[17] X. Li, S. Ganeshan, J. H. Pixley, and S. Das Sarma, Many-Body Localization and Quantum Nonergodicity in a Model with a Single-Particle Mobility Edge, Phys. Rev. Lett. **115**, 186601 (2015).

[18] R. Modak and S. Mukerjee, Many-Body Localization in the Presence of a Single-Particle Mobility Edge, Phys. Rev. Lett. **115**, 230401 (2015).

[19] X. Li, J. H. Pixley, D.-L. Deng, S. Ganeshan, and S. Das Sarma, Quantum nonergodicity and fermion localization in a system with a single-particle mobility edge, Phys. Rev. B **93**, 184204 (2016).

[20] Y.-T. Hsu, X. Li, D.-L. Deng, and S. Das Sarma, Machine Learning Many-Body Localization: Search for the Elusive Nonergodic Metal, Phys. Rev. Lett. **121**, 245701 (2018).

[21] V. Khemani, D. N. Sheng, and D. A. Huse, Two Universality Classes for the Many-Body Localization Transition, Phys. Rev. Lett. **119**, 075702 (2017).

[22] S.-X. Zhang and H. Yao, Universal Properties of Many-Body Localization Transitions in Quasiperiodic Systems, Phys. Rev. Lett. **121**, 206601 (2018).

[23] M. Žnidarič and M. Ljubotina, Interaction instability of localization in quasiperiodic systems, Proc. Natl. Acad. Sci. U.S.A. **115**, 4595 (2018).

[24] E. V. H. Doggen and A. D. Mirlin, Many-body delocalization dynamics in long Aubry-André quasiperiodic chains, Phys. Rev. B **100**, 104203 (2019).

[25] S. Xu, X. Li, Y.-T. Hsu, B. Swingle, and S. Das Sarma, Butterfly effect in interacting Aubry-Andre model: Thermalization, slow scrambling, and many-body localization, Phys. Rev. Res. **1**, 032039(R) (2019).

[26] F. A. An, K. Padavić, E. J. Meier, S. Hegde, S. Ganeshan, J. H. Pixley, S. Vishveshwara, and B. Gadway, Interactions and Mobility Edges: Observing the Generalized Aubry-André Model, Phys. Rev. Lett. **126**, 040603 (2021).

[27] Y. Wang, J.-H. Zhang, Y. Li, J. Wu, W. Liu, F. Mei, Y. Hu, L. Xiao, J. Ma, C. Chin, and S. Jia, Observation of Interaction-Induced Mobility Edge in an Atomic Aubry-André Wire, Phys. Rev. Lett. **129**, 103401 (2022).

[28] P. Roushan, C. Neill, J. Tangpanitanon, V. M. Bastidas, A. Megrant, R. Barends, Y. Chen, Z. Chen, B. Chiaro, A. Dunsworth, A. Fowler, B. Foxen, M. Giustina, E. Jeffrey, J. Kelly, E. Lucero, J. Mutus, M. Neeley, C. Quintana, D. Sank *et al.*, Spectroscopic signatures of localization with interacting photons in superconducting qubits, Science **358**, 1175 (2017).

[29] T. Kohlert, S. Scherg, X. Li, H. P. Lüschen, S. Das Sarma, I. Bloch, and M. Aidelsburger, Observation of Many-Body Localization in a One-Dimensional System with a Single-Particle Mobility Edge, Phys. Rev. Lett. **122**, 170403 (2019).

[30] S. Yao and Z. Wang, Edge States and Topological Invariants of Non-Hermitian Systems, Phys. Rev. Lett. **121**, 086803 (2018).

[31] V. M. Martinez Alvarez, J. E. Barrios Vargas, and L. E. F. Foa Torres, Non-Hermitian robust edge states in one dimension: Anomalous localization and eigenspace condensation at exceptional points, Phys. Rev. B **97**, 121401(R) (2018).

[32] F. K. Kunst, E. Edvardsson, J. C. Budich, and E. J. Bergholtz, Biorthogonal Bulk-Boundary Correspondence in Non-Hermitian Systems, Phys. Rev. Lett. **121**, 026808 (2018).

[33] K. Yokomizo and S. Murakami, Non-Bloch Band Theory of Non-Hermitian Systems, Phys. Rev. Lett. **123**, 066404 (2019).
[34] C. H. Lee and R. Thomale, Anatomy of skin modes and topology in non-Hermitian systems, Phys. Rev. B **99**, 201103(R) (2019).
[35] S. Longhi, Probing non-Hermitian skin effect and non-Bloch phase transitions, Phys. Rev. Res. **1**, 023013 (2019).
[36] D. S. Borgnia, A. J. Kruchkov, and R.-J. Slager, Non-Hermitian Boundary Modes and Topology, Phys. Rev. Lett. **124**, 056802 (2020).
[37] N. Okuma, K. Kawabata, K. Shiozaki, and M. Sato, Topological Origin of Non-Hermitian Skin Effects, Phys. Rev. Lett. **124**, 086801 (2020).
[38] K. Zhang, Z. Yang, and C. Fang, Correspondence between Winding Numbers and Skin Modes in Non-Hermitian Systems, Phys. Rev. Lett. **125**, 126402 (2020).
[39] K. Kawabata, N. Okuma, and M. Sato, Non-Bloch band theory of non-Hermitian Hamiltonians in the symplectic class, Phys. Rev. B **101**, 195147 (2020).
[40] C. Scheibner, W. T. M. Irvine, and V. Vitelli, Non-Hermitian Band Topology and Skin Modes in Active Elastic Media, Phys. Rev. Lett. **125**, 118001 (2020).
[41] Y. Yi and Z. Yang, Non-Hermitian Skin Modes Induced by On-Site Dissipations and Chiral Tunneling Effect, Phys. Rev. Lett. **125**, 186802 (2020).
[42] L. Li, C. H. Lee, S. Mu, and J. Gong, Critical non-Hermitian skin effect, Nat. Commun. **11**, 5491 (2020).
[43] K. Zhang, Z. Yang, and C. Fang, Universal non-Hermitian skin effect in two and higher dimensions, Nat. Commun. **13**, 2496 (2022).
[44] Y.-C. Wang, J.-S. You, and H. H. Jen, A non-Hermitian optical atomic mirror, Nat. Commun. **13**, 4598 (2022).
[45] T. Helbig, T. Hofmann, S. Imhof, M. Abdelghany, T. Kiessling, L. W. Molenkamp, C. H. Lee, A. Szameit, M. Greiter, and R. Thomale, Generalized bulk–boundary correspondence in non-Hermitian topolectrical circuits, Nat. Phys. **16**, 747 (2020).
[46] T. Hofmann, T. Helbig, F. Schindler, N. Salgo, M. Brzezińska, M. Greiter, T. Kiessling, D. Wolf, A. Vollhardt, A. Kabaši, C. H. Lee, A. Bilušić, R. Thomale, and T. Neupert, Reciprocal skin effect and its realization in a topolectrical circuit, Phys. Rev. Res. **2**, 023265 (2020).
[47] A. Ghatak, M. Brandenbourger, J. van Wezel, and C. Coulais, Observation of non-Hermitian topology and its bulk–edge correspondence in an active mechanical metamaterial, Proc. Natl. Acad. Sci. U.S.A. **117**, 29561 (2020).
[48] S. Weidemann, M. Kremer, T. Helbig, T. Hofmann, A. Stegmaier, M. Greiter, R. Thomale, and A. Szameit, Topological funneling of light, Science **368**, 311 (2020).
[49] L. Xiao, T. Deng, K. Wang, G. Zhu, Z. Wang, W. Yi, and P. Xue, Non-Hermitian bulk–boundary correspondence in quantum dynamics, Nat. Phys. **16**, 761 (2020).
[50] L. Xiao, T. Deng, K. Wang, Z. Wang, W. Yi, and P. Xue, Observation of Non-Bloch Parity-Time Symmetry and Exceptional Points, Phys. Rev. Lett. **126**, 230402 (2021).
[51] L. Zhang, Y. Yang, Y. Ge, Y.-J. Guan, Q. Chen, Q. Yan, F. Chen, R. Xi, Y. Li, D. Jia, S.-Q. Yuan, H.-X. Sun, H. Chen, and B. Zhang, Acoustic non-Hermitian skin effect from twisted winding topology, Nat. Commun. **12**, 6297 (2021).
[52] Q. Lin, T. Li, L. Xiao, K. Wang, W. Yi, and P. Xue, Observation of non-Hermitian topological Anderson insulator in quantum dynamics, Nat. Commun. **13**, 3229 (2022).
[53] Q. Liang, D. Xie, Z. Dong, H. Li, H. Li, B. Gadway, W. Yi, and B. Yan, Dynamic Signatures of Non-Hermitian Skin Effect and Topology in Ultracold Atoms, Phys. Rev. Lett. **129**, 070401 (2022).
[54] Q. Lin, T. Li, L. Xiao, K. Wang, W. Yi, and P. Xue, Topological Phase Transitions and Mobility Edges in Non-Hermitian Quasicrystals, Phys. Rev. Lett. **129**, 113601 (2022).
[55] N. Hatano and D. R. Nelson, Localization Transitions in Non-Hermitian Quantum Mechanics, Phys. Rev. Lett. **77**, 570 (1996).
[56] S. Mu, C. H. Lee, L. Li, and J. Gong, Emergent Fermi surface in a many-body non-Hermitian fermionic chain, Phys. Rev. B **102**, 081115(R) (2020).
[57] F. Alsallom, L. Herviou, O. V. Yazyev, and M. Brzezińska, Fate of the non-Hermitian skin effect in many-body fermionic systems, Phys. Rev. Res. **4**, 033122 (2022).
[58] K. Kawabata, T. Numasawa, and S. Ryu, Entanglement Phase Transition Induced by the Non-Hermitian Skin Effect, Phys. Rev. X **13**, 021007 (2023).
[59] R. Hamazaki, K. Kawabata, and M. Ueda, Non-Hermitian Many-Body Localization, Phys. Rev. Lett. **123**, 090603 (2019).
[60] L.-J. Zhai, S. Yin, and G.-Y. Huang, Many-body localization in a non-Hermitian quasiperiodic system, Phys. Rev. B **102**, 064206 (2020).
[61] K. Suthar, Y.-C. Wang, Y.-P. Huang, H. H. Jen, and J.-S. You, Non-Hermitian many-body localization with open boundaries, Phys. Rev. B **106**, 064208 (2022).
[62] S. Ganeshan, J. H. Pixley, and S. Das Sarma, Nearest Neighbor Tight Binding Models with an Exact Mobility Edge in One Dimension, Phys. Rev. Lett. **114**, 146601 (2015).
[63] Q.-B. Zeng and Y. Xu, Winding numbers and generalized mobility edges in non-Hermitian systems, Phys. Rev. Res. **2**, 033052 (2020).
[64] Q. Guo, C. Cheng, Z.-H. Sun, Z. Song, H. Li, Z. Wang, W. Ren, H. Dong, D. Zheng, Y.-R. Zhang, R. Mondaini, H. Fan, and H. Wang, Observation of energy-resolved many-body localization, Nat. Phys. **17**, 234 (2021).
[65] Q. Guo, C. Cheng, H. Li, S. Xu, P. Zhang, Z. Wang, C. Song, W. Liu, W. Ren, H. Dong, R. Mondaini, and H. Wang, Stark Many-Body Localization on a Superconducting Quantum Processor, Phys. Rev. Lett. **127**, 240502 (2021).
[66] W. Morong, F. Liu, P. Becker, K. S. Collins, L. Feng, A. Kyprianidis, G. Pagano, T. You, A. V. Gorshkov, and C. Monroe, Observation of Stark many-body localization without disorder, Nature (London) **599**, 393 (2021).
[67] L. Su, C.-X. Guo, Y. Wang, L. Li, X. Ruan, Y. Du, S. Chen, and D. Zheng, Observation of size-dependent boundary effects in non-Hermitian electric circuits, Chin. Phys. B **32**, 038401 (2023).
[68] W. Zhang, F. Di, H. Yuan, H. Wang, X. Zheng, L. He1, H. Sun, and X. Zhang, Observation of non-Hermitian many-body skin effects in Hilbert space, arXiv:2109.08334.
[69] Z. Gong, Y. Ashida, K. Kawabata, K. Takasan, S. Higashikawa, and M. Ueda, Topological Phases of Non-Hermitian Systems, Phys. Rev. X **8**, 031079 (2018).
[70] See Supplemental Material http://link.aps.org/supplemental/10.1103/PhysRevB.107.L220205 for the details of numerical procedure, influence of NHSE at extremely large non-

Hermiticity, dynamical properties at infinite-time limit, and different disorder strengths.

[71] B. Bauer and C. Nayak, Area laws in a many-body localized state and its implications for topological order, J. Stat. Mech. (2013) P09005.

[72] Y. O. Nakagawa, M. Watanabe, H. Fujita, and S. Sugiura, Universality in volume-law entanglement of scrambled pure quantum states, Nat. Commun. **9**, 1635 (2018).

[73] A. J. Daley, Quantum trajectories and open many-body quantum systems, Adv. Phys. **63**, 77 (2014).